MBE GROWTH CONSIDERATIONS FOR THE FABRICATION OF 640X480 IR FOCAL PLANE ARRAYS OF SiGe HIP DETECTORS

P. E. THOMPSON*, M. WEEKS**, P. TEDROW***, and K. HOBART*
*Code 6812, Naval Research Laboratory, Washington, DC 20375, thompson@estd.nrl.navy.mil
**Rome Laboratory, Hanscom AFB, MA,
***PML, Lowell, MA

ABSTRACT

Encouraging results have been reported for discrete heterojunction internal photoemission (HIP) infrared (IR) detectors composed of heavily boron doped $Si_{1-x}Ge_x$ layers on Si. We desired to build on those results and fabricate 640x480 IR focal plane arrays on 100 mm Si substrates, suitable for commercial microelectronic processing. In this paper we discuss the growth issues for growing these structures by molecular beam epitaxy. Since the wafers had already undergone processing and some had PtSi contacts, the growth temperature was constrained to be no greater than 600 °C. Precise temperature control was obtained by calibrating an optical pyrometer with a thermocouple embedded in the substrate heater assembly, which was calibrated using the eutectic temperatures of Au/Si and Al/Si. The final step of the cleaning process was a 1% HF dip/ spin dry, which resulted in a H-terminated surface. The H was removed at 550 °C in vacuum prior to growth. The growth of the B-doped SiGe layer was done at 350 °C to minimize segregation and diffusion of the Ge and B. Doping levels of $2x10^{20}/cm^3$ were obtained with near 100% activation. Using $Si_{0.65}Ge_{0.35}$, doped with $2x10^{20}$ B/cm^3, a cut-off wavelength of 11.1 µm and an emission coefficient of 19.8 %/eV were obtained for discrete detectors. Preliminary results from the detector arrays show full functionality in the spectral range of 6.1 to 12.8 µm.

INTRODUCTION

There is great interest in developing infrared (IR) detectors for the atmospheric transparent wavelength windows of 2 - 6 µm and 8 - 14 µm. While IR detectors can be fabricated from compound semiconductors such as InSb (2 - 4 µm) and HgCdTe (8 - 14 µm), it is desirable to investigate Si-based detectors. Detectors fabricated in Si have advantages over other materials in cost, uniformity, ease of fabrication, and monolithic integration. One Si-based device which has been demonstrated to operate in these wavelength regimes is the SiGe/Si heterojunction internal photoemission (HIP) IR detector[1-4]. The HIP detector employs a degenerately doped p^+ $Si_{1-x}Ge_x$ cap layer and a p^- Si substrate. The detection mechanism takes advantage of the energy difference between the valence band of the doped $Si_{1-x}Ge_x$ and Si. The photon is absorbed in the p+ $Si_{1-x}Ge_x$ cap layer and a hole is ejected into the Si collector region. The cutoff wavelength of detection is determined by the difference between the valence band discontinuity of the $Si_{1-x}Ge_x$ and the Si, ΔE_v, and the Fermi level, E_f, in the SiGe layer.

$$\lambda_{cutoff} = hc/E_{barrier} = hc/(\Delta E_v - E_f) \qquad (1)$$

By controlling the Ge concentration, x, and the p-type doping concentration, the cutoff wavelength can be varied from 3 to 30 µm.

The ultimate goal of our project was to fabricate a 480 x 640 detector array of SiGe HIP detectors for absorption at 8 µm, using 4 inch Si wafers and a commercial fabrication facility. The processing sequence required the degenerately doped $Si_{1-x}Ge_x$ to be grown on partially processed wafers having both Pt-silicide contacts and patterned oxide on the surface. In this paper we will address the specific constraints on the molecular beam epitaxy (MBE) growth process, discuss

how these constraints were met to successfully fabricate the devices, and report on initial device results

EXPERIMENTAL

The VG-V80 MBE growth system used electron beam evaporation of solid Si and Ge to form the molecular fluxes. The boron flux was obtained from elemental boron using a specially designed Knudsen cell to accommodate the high temperature required to obtain a significant doping concentration. The Pt-silicide contacts on the samples meant that the substrate temperature could not exceed 600 °C during any portion of the growth process. In addition a substantial portion of each wafer surface was covered with SiO_2, which would interfere with the surface temperature measurement using an optical pyrometer. The following specific concerns were addressed:

a. A low temperature ($T \leq 550$ °C) *in situ* cleaning process had to be used so that the surface was atomically clean and ready for epitaxial growth.

b. The temperature of the substrate had to be calibrated and monitored throughout the growth.

c. Boron doping had to be performed at a low growth temperature to minimize dopant and Ge segregation.

d. Both the Si and Ge fluxes had to be well calibrated since λ_{cutoff} is sensitive to x.

In addition to the growth considerations, a technique for the post-growth, *ex situ*, removal of the SiGe deposited on the SiO_2 had to be established.

Ishizaka and Shiraki [5] have developed a cleaning process, commonly known as the "Shiraki" process, which is widely accepted by the Si MBE growth community for the formation of "impurity free" surfaces. The final step in this technique is the formation of a layer of SiO_x, which is thermally desorbed in the growth chamber prior to growth at a temperature > 800 °C. The temperature required for the desorption of the volatile oxide makes this process unacceptable for the HIP structures. Low temperature substrate cleaning techniques have been investigated [6-12]. The common factor in all of the studies is that the final step results in a hydrogen terminated surface. It has been demonstrated that this surface is stable in air for several hours [13,14]. The hydrogen on the surface can be desorbed at 550 °C in vacuum, as observed by the burst in chamber pressure. At NRL we have investigated several HF-terminated cleaning processes and compared the results to the Shiraki clean [12]. The surfaces were studied prior to growth using X-ray photoelectron spectroscopy (XPS) and the initial growth interface was analyzed using secondary ion mass spectrometry (SIMS). We concluded that by abbreviating the Shiraki clean by eliminating the wet oxide growth and completing the clean with a 4 % HF, 20 s dip and blow dry with N_2 we could obtain equivalently clean surfaces. For the HIP detector arrays we used the RCA clean [15] followed by a 10% HF, 10 s dip, then a 1% HF, 15 s dip, and then spun the samples dry to produce the hydrogen-terminated surface.

Knowledge of the surface temperature is always critical in any crystal growth process. In the MBE growth system the temperature was monitored by two techniques. There is a W-5%Re/W-26%Re thermocouple embedded in the deposition stage heater, located approximately 2 cm from the substrate. The blackbody emission from the substrate is monitored by an optical pyrometer. Neither technique is an absolute measure of the surface temperature. Since the thermocouple is attached to the heater assembly, the thermal mass of the stage causes considerable lag time (~ 10 min.) until an equilibrium temperature is reached. Even then the temperature measured by the thermocouple is at best related to the sample temperature by some unknown function because of the distance between the two. The pyrometer temperature has a fast response time, but the emissivity of the surface must be known. We have calibrated the temperature employing the eutectic temperature of Au on Si (363 °C) and Al on Si (577 °C) as standards [16]. A 200 nm film of Au or Al was evaporated unto a hydrogen-terminated Si wafer through an Al foil shadow mask. The calibration wafer had a maximum of 10% metal coverage, with the center of the wafer kept clear for pyrometer measurements. The wafer is then slowly heated to the eutectic temperature. The transition is observed as an abrupt change in the reflectivity of the deposited

metal as it is dissolved into the Si. The emissivity of the Si wafer is then chosen as that value which makes the real temperature and the temperature measured by the pyrometer nearly equal at 550 °C. Using a clean Si substrate, the substrate was taken from 300 °C to 700 °C in a series of steady state steps to determine the equivalent temperatures between the thermocouple and the pyrometer. The temperature calibration is dependent upon the doping concentration and surface of the wafer. The temperature calibration for the substrate for the HIP structure is shown in Fig. 1. It is seen that a real temperature of 550 °C corresponds to a pyrometer temperature of 590 and a thermocouple temperature of 660.

The SiGe layers must be degenerately doped with boron. It has been reported [3] that good surface morphology and low misfit dislocation density was observed when the growth temperature was kept at 350 °C. We had calibrated the boron doping cell (carrier concentration versus k-cell temperature) for a growth rate of Si of 0.1 nm/s at a substrate growth temperature of 500 °C, Fig. 2, using Hall measurements. The uniformity of the doping across the wafer was verified by manually mapping the sheet resistance with a four point probe. When 40 nm test layers of $Si_{0.7}Ge_{0.3}$ were grown at 0.1 nm/s at temperatures of 350, 425, and 550 °C with the boron cell set at 1900 °C, the Hall measurements revealed no differences in either the carrier concentration or in the mobility as a function of growth temperature. The Hall carrier concentration was a factor of 4 higher for the SiGe alloy than for Si, which may, in part, be accounted for by a difference in the Hall factor for the two materials [17]. Since we wanted degenerate p-type doping, we were not concerned about this result and did not pursue it further.

The cutoff wavelength is determined by composition (x) of the $Si_{1-x}Ge_x$ cap and the doping concentration. As discussed above, the doping concentration is controlled by the k-cell temperature and is calibrated for a growth-rate of 0.1 nm/s. The growth-rate is determined by the molecular flux of the Si and Ge, which must be known and controlled. We have used an Inficon Sentinel III system to control the e-beam sources. During growth a portion of each flux is intercepted and ionized. The intensity of the excitation photoemission is analyzed, resulting in a feedback signal to increase or decrease the electron current impinging on the Si or Ge source. Calibration of the Sentinel III system is obtained by thickness measurements of elemental films on sapphire wafers measured by surface profilometry and standard epitaxial structures measured with Rutherford backscattering spectroscopy and x-ray diffraction. Using the results from these structures, the photomultiplier voltage in the Sentinal III is adjusted.

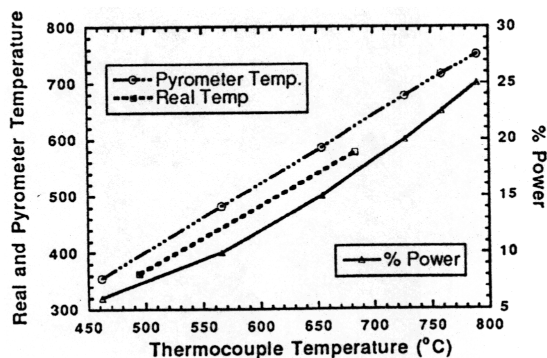

Fig. 1. Temperature calibration for the Si substrate used for the HIP FPA. The real temperatures of the substrate are obtained from the eutectic temperatures of Au/Si and Al/Si. An emissivity value of 0.53 was used for the optical pyrometer.

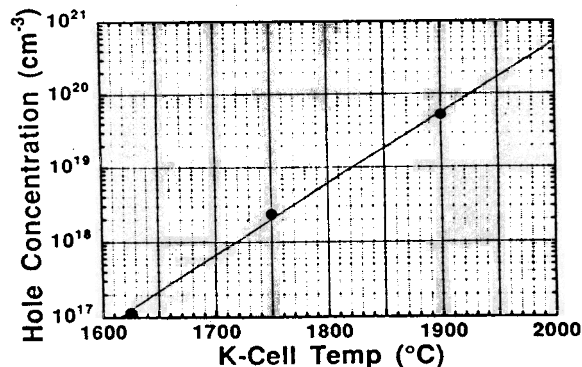

Fig. 2. Hole concentration measured using Hall electrical measurements of 300 nm Si, grown at 500 °C at 0.1 nm/s, doped with boron. The boron K-cell temperature determines the boron molecular flux.

After the growth considerations were addressed, a technique for the post-growth, *ex situ*, removal of the SiGe deposited on the SiO_2 was established. Lithography was performed using an oversized clear field mask. This mask protected the SiGe on the active area as well as the surrounding oxide. The unwanted SiGe was sputtered away in a Plasma Science RIE sputtering system. The fabrication sequence was completed with the deposition and patterning of Al contacts and pads.

DEVICE RESULTS

Prior to the growth of the FPAs, a series of discrete detectors were fabricated and tested to determine the optimum film parameters, Table I. The devices did not have antireflective coatings or surface mirrors to enhance their efficiency since a relative measure of performance was the important factor. Germanium concentration, boron doping concentration, and alloy thickness were varied. The measurement temperature was 40 K unless noted differently in the table. The photoresponse fit the modified Fowler equation [18]

$$Y = C_1(E_{hv} - \varphi_{opt})^2/E_{hv} \qquad (2)$$

where Y is the photoelectric yield in electrons/photon, C_1 is the emission coefficient in $(eV)^{-1}$, E_{hv} is the photon energy in eV, and φ_{opt} is the cutoff energy in eV. The measured Fowler plot data for sample 6.3NRL is presented in Fig. 3. φ_{opt} was obtained from the intercept with the x-axis and C_1 is determined from the slope. A plot of the thermionic emission versus 1/T was used to determine the electrical barrier height, φ_{elec}, and the effective Richardson constant, A** [19]. The electrical and optical measurements were self-consistent. The parameters for 6.3NRL (10 nm $Si_{0.65}Ge_{0.35}$, 2 x 10^{20} B/cm^3, and) were chosen to be optimum for the FPA.

Table I. NRL/RL Test Diodes

ID	Comments	φ_{opt}	C_1(%/eV)	φ_{elec}	A**
19NRL	10 nm $Si_{0.65}Ge_{0.35}$ 5 x 10^{19} B/cm^3 40K	0.310	1.7	0.323	17.1
6.1NRL	5 nm $Si_{0.65}Ge_{0.35}$ 2 x 10^{20} B/cm^3 20K	0.081	20.6	0.069	5.3
6.2NRL	10 nm $Si_{0.65}Ge_{0.35}$ 5 x 10^{19} B/cm^3 40K	0.255	2.3	0.248	79.3
6.3NRL	10 nm $Si_{0.65}Ge_{0.35}$ 2 x 10^{20} B/cm^3 40K	0.105	19.8	0.087	6.1
6.4NRL	10 nm $Si_{0.7}Ge_{0.3}$ 2 x 10^{20} B/cm^3 17K	0.078	21.3	0.059	2.9

Each of the wafers for FPA processing had test diodes. The photoresponse cutoff wavelengths of the discrete detectors on the completed FPA substrates ranged from 7.3 to 12.4 μm (with one unexplained measurement that showed a device with cut off at 41.2 μm). Values for cutoff wavelength were obtained for some of the diodes using thermionic emission and capacitance-voltage methods and were found to be equivalent to those obtained with the Fowler plots.

Thermal imagery was demonstrated with a 640 x 480 FPA device in the spectral range of 6 - 12 μm, Fig. 4. The FPA was mounted in a test dewar cooled with liquid helium to 35 K. The test dewar contained a cooled IR band pass filter limiting the spectral band from 6.1 to 12.8 μm. The cold shield aperture was f/1.0 and the integration time set to 33 ms. The measured thermal response was 1.9 x 10^4 electrons/K at 300 K scene temperature. The saturation signal was

~2 x 10^6 electrons with a detector bias of 5.2 volts, and the cold scene leakage signal of 2 x 10^5 electrons. From the cutoff wavelength measurements of the test diode, it is believed that this device had a cutoff > 12 µm. The thermal imagery showed good contrast for the bright light source, but poorer than expected contrast for hand scenes. It is suspected that this may be due to too much signal from the background driving the detector into soft saturation. More measurements need to be taken before these issues can be resolved.

Fig. 3. Fowler plot for sample 6.3NRL

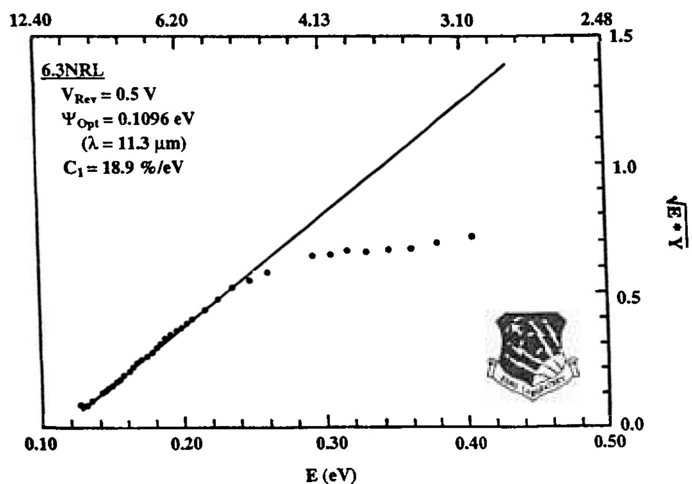

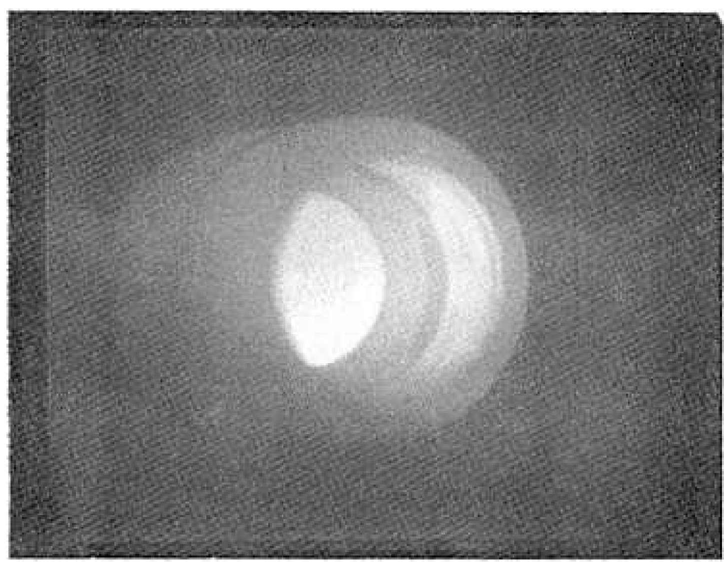

Fig. 4. Thermal imagery taken with 640 x 480 IR FPA (device 10-4-25).

CONCLUSION

Specific MBE growth issues such as a low temperature (T < 550 °C) *in situ* cleaning, temperature calibration of the substrate, and low temperature boron doping were addressed so that 640X480 IR focal plane arrays of SiGe HIP detectors could be fabricated on 100 mm Si wafers at a commercial fabrication facility. Preliminary tests show that the cutoff wavelength of the array is > 12 µm.

ACKNOWLEDGMENTS

The authors wish to recognize the efforts of Mr. Larry Ardis and Dr. Mohammad Fatemi, both of NRL, for MBE sample preparation and X-ray analysis, respectively. The 640x480 FPAs were fabricated and tested at David Sarnoff Research Center, Princeton, NJ by Frank Shallcross, Tom Villani, Dietrich Meyerhofer, and Neil McCaffrey.

REFERENCES

F. D. Shepard, V. E. Vickers, and A. C. Yang, U. S. Patent No. 3,603,847, June 11, 1969.

2. T. L. Lin and J. Maserjian, Appl. Phys. Lett. **57**, 1422 (1990)

3. T. L. Lin, T. George, E. W. Jones, A. Ksendzov, and M. L. Huberman, Appl. Phys. Lett. **60**, 380 (1992).

4. B.-Y. Tsaur, C. K. Chen, and S. A. Marino, IEEE Electron Device Letters **12**, 293 (1991).

5. A. Ishizaka and Y. Shiraki, J. Electrochem. Soc.**133**, 666 (1986).

6. P. J. Grunthaner, F. J. Grunthaner, R. W. Fathauer, T. L. Lin, F. D. Schowengerdt, B. Pate, and J. H. Mazur, in J. C. Bean and L. J. Schowalter (eds.), *Silicon Molecular Beam Epitaxy*, Vol. 88-8, The Electrochemical Society, New Jersey, 1988, p. 375.

7. T. Takahagi, I. Nagai, A. Ishitani, H. Kuroda, and Y. Nagasawa, J. Appl. Phys. **64**, 3516 (1988).

8. D. B. Fenner, D. K. Biegelsen, and R. D. Bringans, J. Appl. Phys. **66**, 419 (1989).

9. P. J. Grunthaner, F. J. Grunthaner, R. W. Fathauer, T. L. Lin, M. H. Hecht, L. D. Bell, W. J. Kaiser, F. D. Schowengerdt, and J. H. Mazur, Thin Solid Films **183**, 197 (1989).

10. A. Miyauchi, Y. Inoue, T. Suzuki, and M. Akiyama, Appl. Phys. Lett. **57**, 676 (1990).

11 B. Meyerson, F. J. Himpsel, and K. J. Uram, Appl. Phys. Lett. **57**, 1034 (1990).

12. P. E. Thompson, M. E. Twigg, D. J. Godbey, K. D. Hobart, and D. S. Simons, J. Vac. Sci Technol. B **11**(3) 1077 (1993).

13. N. Hirashita, M. Kinoshita, I. Aikawa, and T. Ajioka, Appl. Phys. Lett. **56**, 452 (1990).

14. G. S. Higashi, Y. J. Chabal, G. W. Trucks, and K. Raghavachari, Appl. Phys. Lett. **56**, 656 (1990).

15. W. Kern and D. A. Puotinen, RCA Review **31**, 105 (1985)

16. *Bulletin of Alloy Phase Diagrams*, American Society for Metals, Metals Park, OH.

17. T. K. Carns, S. K. Chun, M. O. Tanner, K. L. Wang, T. I. Kamins, J. E. Turner, D. Y. C, Lie, M.-A. Nicolet, and R. G. Wilson, IEEE Trans. Electron. Devices **41**, 1273 (1994).

18. V. L. Dalal, J. Appl. Phys. **42**, 2274 (1971).

19. S. M. Sze, *Physics of Semiconductor Devices*, 2nd. ed. (Wiley, New York, 1981), Chap. 5.